Spora: A Journal of Biomathematics

Volume 9 Article 6

2023

Modeling the Population Demographics & Viability of Imperiled Guzmania monostachia Populations

Helen Pennington
Rhodes College, penhe-24@rhodes.edu

Pranay Lingareddy
Rhodes College, pranay.lingareddy2@gmail.com

Erin N. Bodine
Rhodes College, bodinee@rhodes.edu

Modeling the Population Demographics & Viability of Imperiled Guzmania monostachia Populations

Cover Page Footnote

Corresponding author is Erin N. Bodine

Intercollegiate Biomathematics Alliance

SPORA
A Journal of Biomathematics

ISSN 2473-3067 (Print)
ISSN 2473-5493 (Online)

Modeling the Population Demographics & Viability of Imperiled *Guzmania monostachia* Populations

Helen Pennington[1], Pranay Lingareddy[1], Erin N. Bodine[1,*]

*Correspondence:
Dr. Erin N. Bodine, Dept. of Mathematics & Computer Science, Rhodes College, 2000 North Parkway, Memphis, TN 38112, USA
bodinee@rhodes.edu

Abstract

Guzmania monostachia is a large, long-lived bromeliad whose leaves grow in a rosette pattern and is native to the Americas, but endangered in Florida due to damage caused by the invasive weevil *Metamasius callizona*. Each *G. monostachia* rosette can reproduce sexually via flowers or asexually by producing clonal offshoot rosettes. We model the population dynamics and demographic structure of a *G. monostachia* population using a Lefkovitch matrix model where each state represents a demographic class of rosettes. Model analysis over a range of uncertain parameters show the conditions under which a *G. monostachia* population is viable in the absence and presence of *M. callizona*, and the expected demographic structure under those conditions. In particular, our analysis illustrates that proportional reductions in survival have a qualitatively stronger impact on population viability than proportion reductions in clonal fecundity.

Keywords: Lefkovitch matrix, demographic model, *Guzmania monostachia*, population viability

1 Introduction

Guzmania monostachia is a large, long-lived epiphyte in the primarily neotropical plant family Bromeliaceae which contains over 3,000 flowering species commonly referred to as bromeliads. The vegetative bodies of bromeliads grow in a rosette pattern with the newest leaves growing from the center of the rosette. Most bromeliads (including *G. monostachia*) are monocarpic which means that each rosette will produce a single inflorescence (i.e., flowering structure), typically from the center of the rosette, before the rosette desiccates and dies. However, most bromeliads (including *G. monostachia*) are also iteroparous which means that they have multiple opportunities for sexual reproduction via flowers prior to the death of the genetic individual through the production of clonal rosettes. Each *G. monostachia* rosette has the ability to produce clonal rosettes once it has reached a size of 5 cm in longest leaf length (LLL) and will produce, on average, 0.1144 clonal rosettes per year [3]. Therefore, a single genetic *G. monostachia* individual can be comprised of a rosette started from seed and multiple generations of clonal rosettes.

G. monostachia is native to South America, Central America, the West Indies, and Florida [3, 4, 9, 15]. In Florida, *G. monostachia* is one of 16 native bromeliad species, and is one of the 12 bromeliad species classified as endangered in Florida due to an invasive weevil *Metamasius callizona* [8, 9, 15]. The damage caused by *M. callizona* to Florida's native bromeliad populations has been so extensive that the weevil is now colloquially referred to as the "evil weevil" [2, 11].

The invasive *M. callizona* feed on bromeliads throughout their entire life cycle. Adult weevils feed off the leaves of the bromeliad, however, this is not detrimental to the plant [9]. The larvae hatched by the weevil are the primary contributors to the vast decline of the bromeliad population. Female *M. callizona* lay their eggs at the base of bromeliads, preferentially selecting the largest bromeliads. When the larvae hatch, they consume the core of the plant including meristematic tissues. The apical meristem, located at the center of the rosette, is the meristematic tissue responsible for producing new leaves. Once a *G. monostachia* rosette has reached a size of at least 20 cm LLL, the meristematic tissue can go through induction at which point it stops producing new leaves and starts building the inflorescence [3]. The axillary meristems are located above the base of each leaf in the rosette, and are the meristematic tissues responsible for producing clonal rosettes (which can each eventually produce inflorescences of their own). Thus, when the larva consumes the meristematic tissues of a bromeliad, it removes the plant's means of reproduction [9].

In Florida, the three largest native bromeliads, *Tillandsia utriculata*, *Tillandsia fasciculata*, and *G. monostachia* have experienced the most severe population de-

[1]Rhodes College, Department of Mathematics & Computer Science, Memphis, TN

clines due to damage from *M. callizona* larvae. The long generation times of these three bromeliad species have made them slow to rebound in response to rapid weevil predation [7, 9]. All three of these bromeliads are tank-forming, which means that the base of the leaves of the rosette overlap to form a tank that collects rain water. This tank provides an aquatic habitat for many anthropods and frogs [2, 9]. Thus, the decline of these native bromeliad populations will result in the loss of these micro-habitats and species.

To understand and quantify the impact of weevil predation on the demographic structure and population viability of *G. monostachia* we have constructed a demographic model of a population of *G. monostachia* using a stage structured matrix model (presented in Section 2). We analyzed the model to explore the viability of a *G. monostachia* population experiencing reductions in survival and fecundity due to weevil predation (presented in Sections 3 and 4). From our analysis, we can determine which vital statistics should be targeted by conservation strategies for Florida *G. monostachia* populations (presented in Section 5).

2 Mathematical Model

We simulate the population dynamics of *G. monostachia* using a Leftkovich matrix model [6]. The size classes for the stage-structured matrix were determined using the longest leaf length (LLL) of the rosette measured in cm. The model consists of six demographic classes, denoted by $\mathbf{x} = [x_1, \ldots, x_6]^T$ where the size of rosettes in each demographic class are given in Table 1. Time is measured discretely where one time step is equal to one year, and the time step is advanced in late February/early March immediately prior to seed dispersal. Seeds germinate in May [4], and those that survive until next March enter the model in the seedling year 1 class (x_1, 0–0.5 cm LLL). Individual seedling rosettes that survive another year progress to the seedling year 2 class (x_2, 0.5–5 cm LLL). Rosettes remain in the x_2 state for an average of two years [3] before progressing to the medium class (x_3, 5–20 cm LLL) where they remain for an average of two years [3] before progressing to the large class (x_4, >20 cm LLL). Rosettes in the medium and large classes are capable of producing clonal rosettes which grow at a significantly faster rate than rosettes started from seed. The clonal rosettes reach a size of at least 20 cm LLL within one year [3], and subsequently enter the large clonal rosette class (x_6, >20 cm LLL). Once the size of a rosette (either started from seed or a clonal rosette) reaches at least 20 cm LLL, it can go through induction at which point it stops producing new leaves and produces an inflorescence. Large, post-induction rosettes are counted in the x_5 model class where they remain for one time step (one year) before dispersing their seeds and dying.

Table 1: Demographic size/reproductive classes for *G. monostachia* used in Equation (1.1) and depicted in the life-cycle graph in Figure 1.

State Variable	Size/Reproductive Class	LLL (cm)
x_1	Seedling Yr 1	$[0, 0.5]$
x_2	Seedling Yr 2	$[0.5, 5]$
x_3	Medium	$[5, 20]$
x_4	Large (from seed)	>20
x_5	Large (post-induction)	>20
x_6	Large (clonal rosette)	>20

The progression of rosettes through the demographic classes is shown in the life-cycle diagram in Figure 1, and are described by the matrix equation

$$\mathbf{x}(t+1) = \mathbf{A}\mathbf{x}(t) \tag{1.1}$$

where

$$\mathbf{A} = \begin{bmatrix} 0 & 0 & 0 & 0 & ghF_5 & 0 \\ G_1 & P_2 & 0 & 0 & 0 & 0 \\ 0 & G_2 & P_3 & 0 & 0 & 0 \\ 0 & 0 & G_3 & P_4 & 0 & 0 \\ 0 & 0 & 0 & I_4 & 0 & I_6 \\ 0 & 0 & C_3 & C_4 & 0 & C_6 + P_6 \end{bmatrix} \tag{1.2}$$

is a 6×6 Leftkovich matrix in which P_i is the probability that an individual will survive and remain in stage i in the next time step; G_i is the probability that an individual will survive and progress to stage $i+1$ in the next time step; I_i is the probability that an individual will survive and go through induction in the next time step; F_i is the seed fecundity of stage i (i.e., the number of seed produced per rosette); C_i is the clonal fecundity rate of stage i (i.e., the number of clonal rosettes produced per rosette per time step); h is the proportion of seeds produced by a single rosette that disperse to a suitable habitat for germination; and g is the germination rate. The probability that an individual in stage i will survive to the next time step is $S_i = P_i + G_i + I_i$, and ghF_i is the number of seeds that land in a suitable habitat, germinate, and survive one time step to enter the x_1 size class.

Lemma 1. *Let the Lefkovitch matrix* $\mathbf{A}$ *be the 6 × 6 matrix defined in Equation* (1)*. Then* $\mathbf{A}$ *is non-negative, irreducible, and primitive.*

Proof. Let the Lefkovitch matrix $\mathbf{A}$ be the 6×6 matrix defined in Equation (1). Since every entry in $\mathbf{A}$ is non-negative, the matrix is a non-negative matrix. A non-

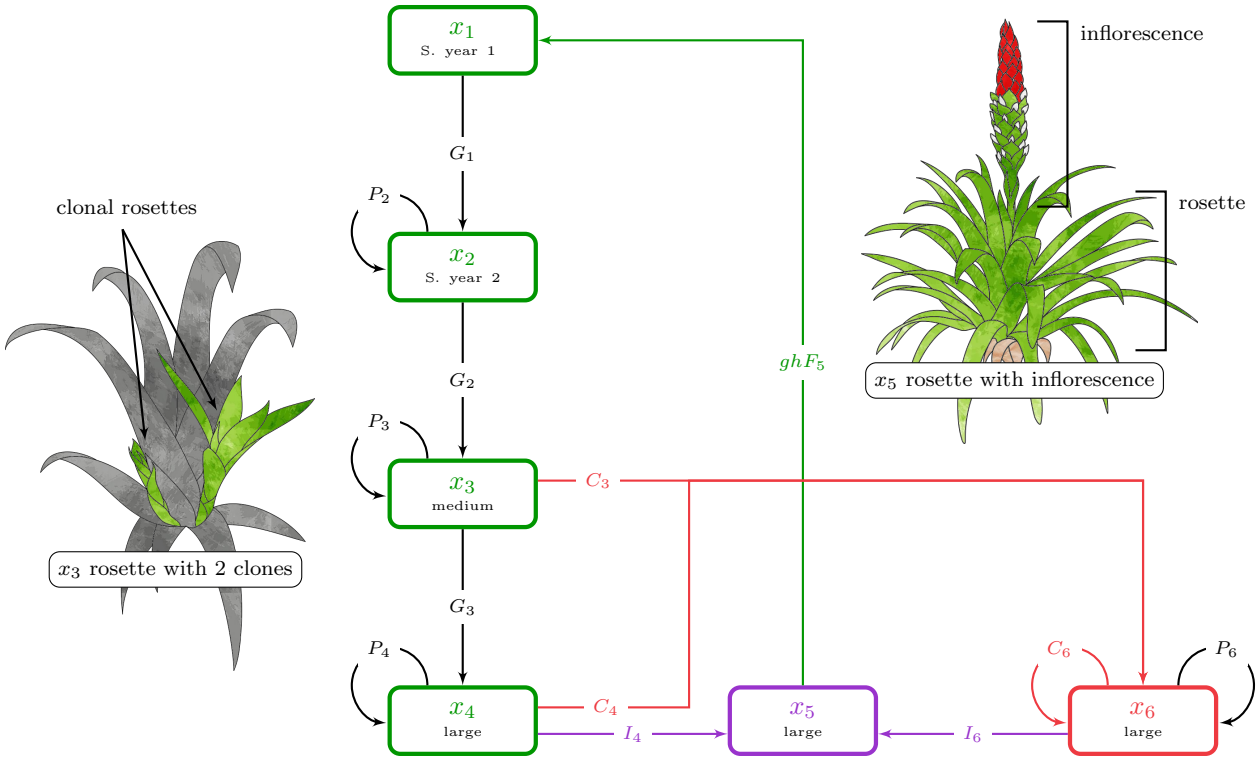

Figure 1: Life-cycle graph corresponding to matrix $\mathbf{A}$ in Equation (1), where ■ = rosettes started from seed, ■ = clonal rosettes, and ■ = post-induction rosettes. Inset sketches show a large rosette with inflorescence (x_5, top right), and a medium rosette (x_3) in the process of producing two clonal rosettes (left) in which the parental rosette is grayed out to accentuate the location of the clonal rosettes.

negative matrix is irreducible if in its life cycle graph representation there exists a path from every node to every other node [6]. The life cycle graph representation of $\mathbf{A}$ in Figure 1 shows that there are no terminal nodes. Thus, there is a path from every node to every other node, and therefore $\mathbf{A}$ is irreducible. An irreducible matrix is primitive if the greatest common divisor of the loop lengths of its life cycle graph is 1, where a loop is a path from a node back to itself [6]. The life cycle graph representation of $\mathbf{A}$ in Figure 1 has loops of length 1, 5, and 6, and thus the greatest common divisor of the loop lengths is 1. Therefore, $\mathbf{A}$ is a primitive matrix.

Theorem 1. *Let* $\mathbf{A}$ *be the* 6×6 *matrix defined in Equation* (1)*. Then there exists a simple, real, and positive eigenvalue* λ_1 *that is greater in magnitude than the other five eigenvalues. Furthermore, the right and left eigenvectors corresponding to* λ_1 *are real and strictly positive.*

Proof. Let $\mathbf{A}$ be the 6×6 matrix defined in Equation (1). Since $\mathbf{A}$ is a square matrix, there are six eigenvalues (denoted λ_i, $i = 1, \ldots, 6$). Each eigenvalue has corresponding left and right eigenvectors (denoted $\mathbf{v}_i$ and $\mathbf{w}_i$, respectively) which satisfy the equations $\lambda_i \mathbf{A} = \mathbf{A}\mathbf{v}_i$ and $\lambda_i \mathbf{A} = \mathbf{w}_i \mathbf{A}$, respectively, for $i = 1, \ldots, 6$. By Lemma 1, $\mathbf{A}$ is irreducible and primitive. Therefore, by the Perron-Frobenius Theorem [6, 10], there exists a simple, real, positive eigenvalue λ_1 that is greater in magnitude than any other eigenvalue (i.e., $\lambda_1 \geq \|\lambda_i\|$ for $i = 2, \ldots, 6$), and its corresponding right and left eigenvectors are real and strictly positive.

Structural equilibrium. A population will be at a structural equilibrium if the proportion of the population in each demographic class remains constant over time. The eigenvector λ_1 from Theorem 1 is referred to as the *dominant eigenvalue* and biologically represents the growth rate of the population at structural equilibrium [6]. If $\lambda_1 > 1$, the population size will grow over time. If $\lambda_1 = 1$, the population size will remain constant over time. If $\lambda_1 < 1$, the population will decrease towards extinction. When considering questions of population viability, we are concerned with the conditions under which $\lambda_1 \geq 1$.

Let $\mathbf{v}_1$ be the normalized right eigenvector corresponding to the dominant eigenvalue (i.e., $\|\mathbf{v}_1\| = 1$). The vector $\mathbf{v}_1$ represents the proportion of the population in each demographic class at structural equilibrium [6]. Populations with high mortality rates in the youngest demo-

graphic classes are expected to have low proportions in the older classes.

Let $\mathbf{w}_1$ be a left eigenvector corresponding to the dominant eigenvalue. The elements of vector $\mathbf{w}_1$ represent the relative reproductive value of each demographic class at structural equilibrium [6]. For the model given in Equation (1), $\mathbf{w}_1$ would represent the relative contribution of each of the six demographic classes towards generating new seedlings entering the seedling year 1 class (x_1). It is common to scale the reproductive values relative to the reproductive value of the smallest or youngest size class [6]. Thus, let $\mathbf{w}_1$ be the left eigenvector such that $\mathbf{w}_1(1) = 1$. Therefore, for the model given in Equation (1) the elements of vector $\mathbf{w}_1$ represent the reproductive value of each demographic class relative to the seedling year 1 class.

2.1 Model parameters

In studies performed in Costa Rica, Cascante-Marín et al. conducted a series of experiments designed to measure various aspects of growth and reproduction in *G. monostachia* and *T. fasciculata* [3, 4]. These studies provided a basis for determining the values of S_i, G_i, P_i, I_i, F_i, C_i, and g for the model given in Equation (1). The value or range of values for each parameter is given in Table 2.

Survival rates (S_i). The probability that an individual rosette in state i at time step t survives to time step $t+1$ is S_i. Estimates and ranges for parameters S_1, S_2, and S_3 were taken from [4]. The range of $S_4 = S_5 = S_6$ has the same upper bound as S_3, but has a lower bound selected such that $P_6 = S_6 - I_6 > 0$. Some rosettes in state i may survive and remain in state i (P_i), while other rosettes in state i will survive and grow into another state (G_i) or survive and induce into the post-induction state (I_i). For each state, $S_i = G_i + P_i + I_i$.

Induction rates (I_i). In the model given in Equation (1), only rosettes in the x_4 and x_6 states can move to the post-induction state (x_5), thus $I_4, I_6 > 0$ and $I_1, I_2, I_3, I_5 = 0$. The range for I_6 is derived directly from data from Cascante-Marín, et al in [3] on the proportion of clonal rosettes (termed "asexual ramets" in [3]) that flowered in their second year, 80–92% of clonal rosettes. Cascante-Marín, et al did not directly report an induction rate for rosettes started from seed (I_4), but did report overall induction rates and total numbers of rosettes (from seed and clonal) with LLL > 20 cm. Thus, the following formulation was used to calculate I_4

$$0.658 = \frac{I_4 x_4 + I_6 x_6}{x_4 + x_6} \Rightarrow I_4 = \frac{0.658(x_4 + x_6) - I_6 x_6}{x_4} \quad (2)$$

Table 2: Parameterization of Equation (1) for NWP *G. monostachia* populations. The values of S_i, G_i, P_i, and I_i are given as a proportion per year; values of C_i are measured as the number of clonal rosettes produced per rosette per year; F_5 is measured in seeds produced per post-induction rosette; g is the probability of germination per seed; and h is a probability.

Parameter	Value or Range	References
S_1	0.148	[4]
S_2	0.527	[4]
S_3	[0.527, 0.960]	[4]
S_4	[0.801, 0.960]	
S_5	[0.801, 0.960]	$S_5 = S_4$
S_6	[0.801, 0.960]	$S_6 = S_4$
G_1	0.148	$G_1 = S_1$
G_2	0.2635	$G_2 = 0.50\, S_2$
G_3	[0.2635, 0.48]	$G_3 = 0.50\, S_3$
P_2	0.2635	$G_2 = 0.50\, S_2$
P_3	[0.2635, 0.48]	$G_3 = 0.50\, S_3$
P_4	[0.285, 0.564]	$P_4 = S_4 - I_4$
P_6	[0.001, 0.16]	$P_6 = S_6 - I_6$
I_4	[0.396, 0.516]	Equation (2)
I_6	[0.80, 0.92]	[3]
C_3	0.1144	[3]
C_4	0.1144	[3]
C_6	0.1144	[3]
F_5	8166	[3]
g	[0.471, 0.514]	[4]
h	[0.01, 1]	

where x_4 and x_6 are the model states for large from seed and large clonal rosette, respectively. Given the range in I_6 values and assuming an equal proportion in states x_4 and x_6, a corresponding range in I_4 was calculated to be 39.6–51.6% of large rosettes started from seed.

Growth & survival rates (G_i and P_i). The probability that an individual rosette in state i at time step t survives and remains in state i is P_i. Note $P_i = 0$ for $i = 1, 5$, because individuals only remain in these states for at most one year (i.e., one time step). The probability that an individual rosette in state i at time step t grows into the next size class $i+1$ by time step $t+1$ is G_i. Note $G_i > 0$ for $i = 1, 2, 3$, and $G_i = 0$ otherwise. The probability that an individual rosette in state i at time step t remains in state i in time step $t+1$ is P_i. Note $P_i > 0$ for $i = 2, 3, 4, 6$, and $P_i = 0$ otherwise.

For $i = 1$, since $I_1 = P_1 = 0$, it follows that $G_1 = S_1$. For $i = 2, 3$, since rosettes spend an average of two

years in the seedling year 2 (x_2) and medium (x_3) states (based on the growth model in Figure 3 of [3]), and since $I_2 = I_3 = 0$, we assume that $G_2 = P_2 = 0.5S_2$ and $G_3 = P_3 = 0.5S_3$. Lastly, since $G_4 = G_6 = 0$, it follows that $P_4 = S_4 - I_4$ and $P_6 = S_6 - I_6$.

Fecundity rates (F_i and C_i). Our model assumes that, of the average seeds produced by a single rosette (F_5), only $g \times h$ of those seeds will survive to the seedling year 1 size class (x_1), where h is the proportion of seeds that land in a suitable habitat and are not eaten/removed prior to germination, and g is the proportion of seeds that germinate and survive one year. An estimate of $F_5 = 8166$ is given in [3], and an estimated range for g is given in [4] (shown in Table 2). There are no known estimates for h, and thus in model analyses we vary the value of h from 0.01 (a scenario in which only 1% of seeds are not removed prior to germination) up to 1.0 (a scenario in which all seeds are viable for germination).

Estimates for C_i values were calculated from measurements from [3] which counted 219 new clonal rosettes produced over three years from a study of 638 rosettes yielding

$$\begin{aligned} C_i &= 219 \text{ clonal rosettes}/638 \text{ rosettes}/3 \text{ yrs} \\ &= 0.1144 \text{ clonal rosettes/rosette/yr.} \end{aligned}$$

Given the lack of data indicating differential clonal fecundity rates for the three different clonal reproductive classes (x_3, x_4, and x_6), we assume $C_i = 0.1144$ for $i = 3, 4, 6$.

3 Model Analysis Methods

3.1 Uncertainty analysis

If a parameter is known to be imprecise or is completely unknown, uncertainty analysis is performed to account for variation in model outcomes due to uncertainty in model parameters. We systematically varied uncertain model parameters to determine the conditions under which a *G. monostachia* population is viable.

Seed dispersal. The seeds of a *G. monostachia* are dispersed via wind [5, 12]. As an epiphyte, *G. monostachia* seeds must land on another plant (typically a tree) in order to germinate. However, the seeds do not always land in a suitable location for germination. In the model given in Equation (1.1), the parameter h defines the proportion of seeds that land in a location suitable for germination. However, there are no known estimates for h, and thus we vary the value of h from 0.01 up to 1.0, and calculate the resulting dominant eigenvalue.

Weevil redation. Exact data could not be found for the magnitude to which weevil predation has reduced the Florida population of *G. monostachia* overtime. In the model, weevil predation was simulated through a proportional reduction of the survival rates of the larger size classes (S_3, S_4, S_5, and S_6), which are the most susceptible to weevil predation. For $i = 4$ and $i = 6$, the inequality $P_i = S_i - I_i > 0$ must be maintained, and thus we proportionally reduced the induction rates I_4 and I_6 by the same amount as the survival rates. Additionally, as noted before, weevil predation occurs mainly through larvae feeding on the meristamatic tissue of *G. monostachia* which affects the production of an inflorescence and the production of clonal rosettes for individual rosettes that otherwise survive predation. To capture the potential impact on the production of clonal rosettes, we also considered a proportional reduction of the clonal fecundity parameters (C_3, C_4, C_6).

Latin hypercube sampling (LHS). Latin hypercube sampling (LHS) is an efficient sampling method for generating parameter sets across a multidimensional parameter space [1, 13]. LHS generates n equiprobable samples from the distribution of each parameter independently without replacement, and then creates n random combinations of sampled parameter values (which we will refer to as parameter sets). We used LHS to generate $n = 1000$ random parameter sets across the parameter space for nine uncertain parameters (S_3, S_4, S_5, S_6, I_4, I_6, P_4, P_6, and g) over the ranges given in Table 2. However, given that $P_6 = S_6 - I_6$, the values of P_6 have the possibility of being negative for some parameter sets. This would not make sense in a biological context, so we used the Constrained LHS (cLHS) algorithm by Petelet et al. [14], which consists of performing a series of permutations on an initial LHS to enforce a desired monotonic constraint ($S_6 > I_6$, in our case). The details of the algorithm are provided in the Appendix.

3.2 Measured outcomes

To determine the conditions for viability of a population of *G. monostachia* in both the presence and absence of weevil predation, we are primarily concerned with the conditions under which $\lambda_1 \geq 1$, where λ_1 is the dominant eigenvalue of $\mathbf{A}$ from Equation (1). Given the parameter values and ranges in Table 2, we used LHS and cLHS to formulate 1000 unique parameter sets. The matrix $\mathbf{A}$ was parameterized for each of the 1000 unique parameter sets, for each value of $h = 0.01, 0.02, \ldots, 1$, and for combinations of proportional reductions in survival rates and clonal fecundity rates ranging from 0% reductions to 90% reductions. The dominant eigenvalue was calculated for each parameterization of matrix $\mathbf{A}$ by solving

$\det(\mathbf{A} - \lambda_1\mathbf{I}) = 0$ for λ_1 (the eigenvalue of greatest magnitude for a single parameterization) where $\mathbf{I}$ is the 6×6 identity matrix.

For four select combinations of h and % reduction in survival and clonal fecundity, we also recorded the range of $\mathbf{v}_1$ and $\mathbf{w}_1$ across 1000 unique parameters sets (determined via LHS and cLHS). Recall from Section 2, $\mathbf{v}_1$ is the the normalized right eigenvector associated with the dominant eigenvalue corresponding to the proportion of the population in each model state at the structural equilibrium, and $\mathbf{w}_1$ is the scaled left eigenvector associated with the dominant eigenvalue corresponding to the reproductive value of each class at structural equilibrium relative to the seedling year 1 class reproductive value. The four select combinations are (1) $h = 1$ and no reduction in survival or clonal fecundity, (2) $h = 0.02$ and no reduction in survival or clonal fecundity, (3) $h = 0.02$ and 30% reduction in survival and clonal fecundity, and (4) $h = 0.02$ and 50% reduction in survival and clonal fecundity.

4 Results

To determine the conditions of population viability for *G. monostachia*, we examined the conditions under which the dominant eigenvalue (λ_1) of $\mathbf{A}$ from Equation (1) was greater than or equal to 1.

Figure 2 shows the impact of varying the parameter h, the proportion of seeds produced by a single rosette that disperse to a location suitable for germination, with different levels of proportional reduction in survival and clonal reproduction. Each graph in Figure 2 shows the mean (black curve) and range (shaded region) of the dominant eigenvalue over the 1000 unique parameter sets. In the case with no reduction in survival or clonal reproduction (Figure 2a) and in the case with no reduction in survival and a 90% reduction in clonal fecundity (Figure 2b, top curves), the entire range of the dominant eigenvalue remains above 1 for all values of $h \geq 0.02$ indicating that even very low levels of seed dispersal to suitable locations will result in viable populations. In the case with a 90% reduction in survival and no reduction in clonal fecundity (Figure 2b, middle curves), the entire range of the dominant eigenvalue is above 1 for all values of $h \geq 0.40$. Thus, if the probability of seeds dispersing to a suitable habitat for germination is low (below 40%) and survival is significantly reduced due to weevil predation, we would expect the *G. monostachia* population to decline to extinction. Lastly, in the case where there is a 90% reduction in both survival and clonal reproduction, the entire range of the dominant eigenvalue is below 1 for all values of h (Figure 2b, bottom curves). Thus, if weevil predation significantly reduces both survival and clonal fecundity, there are no conditions under which the population will remain viable.

To further quantify the relationship between the proportional reduction in survival and clonal fecundity on population viability, we examined the range of two outputs for all combinations of proportional reductions in survival rates and proportional reductions in clonal fecundity rates ranging from 0% reductions to 90% reductions in increments of 0.1% (Figure 3). First, we examined the range in the dominant eigenvalue (λ_1) given 1000 unique parameter sets (determined via LHS and cLHS with parameter ranges given in Table 2) for $h = 0.02$. A value of $h = 0.02$ was used because it was the smallest value of h for which the entire range of the dominant eigenvalue was greater than 1 when there was no reduction in survival rates or clonal fecundity (as shown in Figure 2a). Figures 3a–c show heat maps of the min (Figure 3a), mean (Figure 3b), and max (Figure 3c) dominant eigenvalue for each proportional reduction combination. For each heat map, the cool colors show $\lambda_1 > 1$ (i.e., the population will grow over time and thus is viable over the long term). Second, we examined the range in the minimum proportion of seeds that must land in a suitable location for germination (min h) such that the population is viable ($\lambda_1 > 1$). Figures 3d–f show heat maps of the minimum value of h such that $\min(\lambda_1) > 1$ (Figure 3d), $\text{mean}(\lambda_1) > 1$ (Figure 3e), and $\max(\lambda_1) > 1$ (Figure 3f). When the reduction in survival rates is 40% or less, the minimum h such that $\min(\lambda_1) > 1$ is always less than 0.1. Thus, for these low to moderate reductions in survival rates, the population will remain viable even if the proportion of seeds that land in suitable locations during dispersal are low (around 10%). However, as the reduction in survival rates increases, larger values of h (lighter colors in Figures 3d–f) are required to maintain population viability. When the reduction in survival is 90% and the reduction in clonal fecundity is high (70%, 80% or 90%), there is no value of h such that $\min(\lambda_1) > 1$. These are shown as black squares in Figure 3f. Both sets of heat maps clearly illustrate that proportional reductions in survival have a qualitatively stronger, negative impact on the viability of a *G. monostachia* population than proportional reductions in clonal fecundity.

Lastly, we examined the range of the population proportions at structural equilibrium ($\mathbf{v}_1$), the relative reproductive values for each demographic class at structural equilibrium ($\mathbf{w}_1$), and the dominant eigenvalue (λ_1) given 1000 unique parameter sets (determined via LHS and cLHS with parameter ranges given in Table 2) for four different scenarios: (1) $h = 1$ and no reduction in survival or clonal fecundity (Figures 4a–c), (2) $h = 0.02$ and no reduction in survival or clonal fecundity (Figures 4d–f), (3) $h = 0.02$ and 30% reduction in survival and clonal fecundity (Figures 4g–i), and (4) $h = 0.02$ and 50% re-

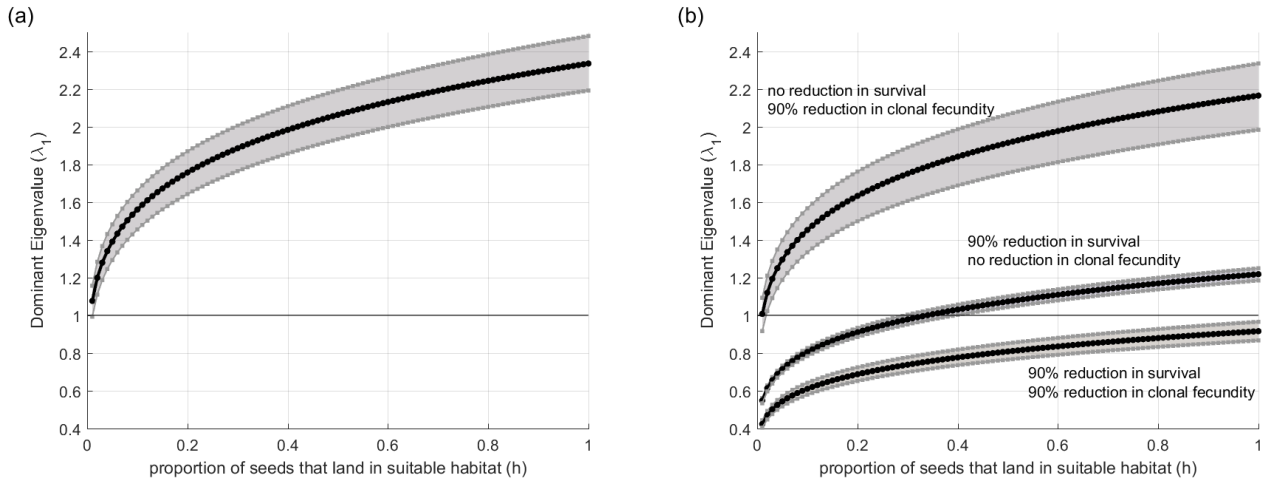

Figure 2: Mean (black) and range (gray) of dominant eigenvalue over 1000 unique parameter sets for the proportion of seeds that land in suitable habitat (h) ranging from 0.01 to 1 given (a) no reduction in survival or clonal reproduction, (b) no reduction in survival with 90% reduction in clonal reproduction (top curves), 90% reduction in survival with no reduction in clonal reproduction (middle curves), and 90% reduction in both survival and clonal reproduction (bottom curves).

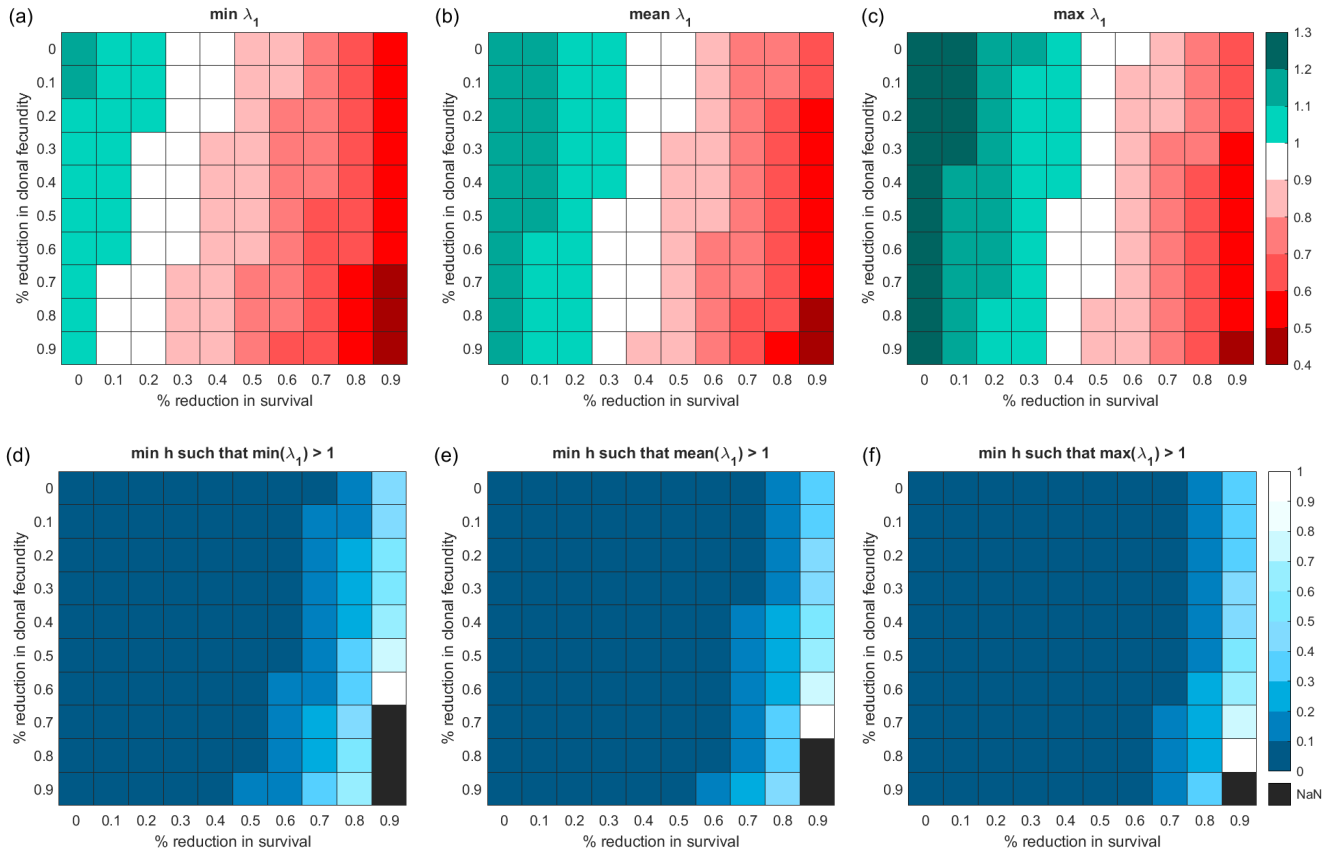

Figure 3: Impact of variation in percent reduction in survival and percent reduction in clonal fecundity. Panels (a)–(c) show range of the dominant eigenvalue (λ_1) over 1000 unique parameter sets given $h = 0.02$ showing (a) min λ_1, (b) mean λ_1, and (c) max λ_1. The cool colors show $\lambda_1 > 1$. Panels (d)–(f) show range of minimum value of h such that (d) min(λ_1) > 1, (e) mean(λ_1) > 1, and (f) max(λ_1) > 1.

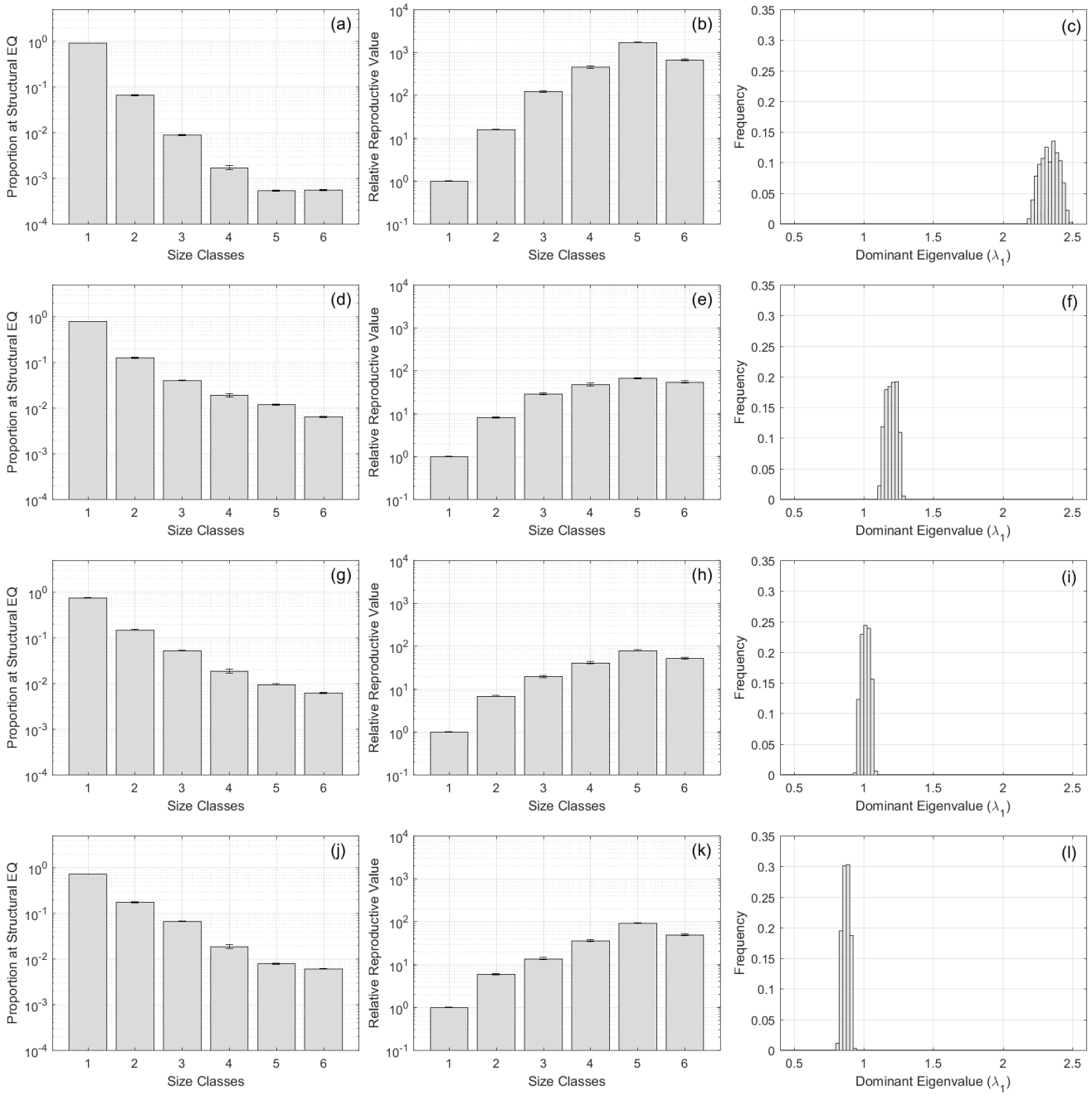

Figure 4: Range in structural equilibrium (left column), relative reproductive value vector (middle column), and dominant eigenvalue (right column) across 1,000 unique parameters sets given $h = 1$ and no reduction in survival or clonal reproduction (a–c), $h = 0.02$ and no reduction in survival or clonal reproduction (d–f), $h = 0.02$ and 30% reduction in survival and clonal reproduction (g–i), and $h = 0.02$ and 50% reduction in survival and clonal reproduction (j–l). Size classes 1, 2, 3, 4, 5, and 6 correspond respectively to seedling year 1, seedling year 2, medium size class, large size class, post-induction size class, and clonal rosettes.

duction in survival and clonal fecundity (Figures 4j–l). Lowering the value of h from 1 to 0.02 results in larger proportions of a *G. monostachia* population residing in the larger demographic classes ($x_2, \ldots, x_6$; compare Figures 4a and 4d), and lower relative reproductive values of those same larger demographic classes (compare Figures 4b and 4e). However, reductions in survival and clonal reproduction do not dramatically change the demographic structure at structural equilibrium ($\mathbf{v}_1$; compare Figure 4d to Figures 4g and 4j) or the relative reproductive value of each demographic class ($\mathbf{w}_1$; compare Figure 4e to Figures 4h and 4k). Across all four scenarios, at structural equilibrium, the largest proportions of the population are in the seedling year 1 and seedling year 2 classes, and the large size classes (x_4, x_5, and x_6) have the highest reproductive value.

In the first scenario when $h = 1$ and there is no reduction in survival and clonal reproduction, the dominant eigenvalue (λ_1) has values in $[2.1, 2.5]$ for all 1000 unique parameter sets (Figure 4c), and thus the population is growing for all parameter sets. In the second scenario when the value of h is lowered to 0.02 (and there is still no reduction in survival and clonal reproduction), $\lambda_1 \in [1.1, 1.3]$ for all 1000 unique parameter sets (Figure 4f). In this case, the population is growing for all parameter sets, but growing slower than in the first scenario. In the third scenario with $h = 0.02$ and 30% reduction in survival and clonal fecundity, $\lambda_1 \in [0.94, 1.1]$ for all 1000 unique parameter sets (Figure 4i). In fact, 35.5% of the parameter sets result in $\lambda_1 < 1$. Thus, if weevil predation is causing a 30% reduction in survival rates and clonal fecundity, then there are parameter scenarios which would lead to the eventual extinction of the *G. monostachia* population under weevil predation. Lastly, in the fourth scenario with $h = 0.02$ and 50% reduction in survival and clonal fecundity, $\lambda_1 \in [0.81, 0.93]$ for all 1000 unique parameter sets (Figure 4l). Thus, in this case, all parameter scenarios result in the *G. monostachia* population declining to extinction.

5 Conclusions

G. monostachia is a large, long-lived ephyphtic bromeliad that is currently listed as endangered in Florida due to the destructive impact of an invasive weevil *M. callizona*. We developed a novel demographic model of a *G. monostachia* population using a stage structured matrix model and parameterized the model using data taken from *G. monostachia* populations in Costa Rica [3, 4]. Due to uncertainty in some of the parameter values, we analyzed model predictions over a range of different survival rates and induction rates. Matrix population theory was used to analyze the long-term yearly growth rate, demographic structure at structural equilibrium, and relative reproductive value for each demographic class.

Weevil predation occurs mainly through larvae feeding on the meristematic tissues of *G. monostachia* and other large bromeliads. Severe damage to the core of the rosette can cause pre-reproductive death (i.e., a reduction in survival). Less severe damage may not kill the rosette, but may damage the apical meristem (preventing sexual reproduction and thus reducing the induction rate) or the axillary meristems (preventing clonal reproduction and thus reducing the clonal fecundity rate). However, each rosette has many axillary meristems (as many as there are leaves), and if one is damaged it would not prohibit the other axillary meristems from initiating and producing clonal rosettes.

Our model analysis shows that reductions in survival rates have a qualitatively greater impact on reducing the population growth rate (and thus the population viability) compared to reductions in clonal fecundity. Reductions in clonal fecundity often had little to no impact on population viability in our model simulations, while reductions in survival rates in all simulations resulted in substantial decreases in the dominant eigenvalue, which when below 1 predict population extinction. However, it should be noted that within our analysis reductions in survival rates (S_i) were coupled with reductions in induction rates (I_i), and thus simulated both a reduction in survival and a reduction in sexual reproduction. The results of our model suggest that conservation efforts will have greater impact if they focus on strategies that increase *G. monostachia* survival rates. Nonetheless, conservation efforts that mitigate damage to meristemic tissue or prevent weevil infestations of *G. monostachia* will likely result in returning populations to baseline (pre-weevil infestation) survival rates and clonal fecundity rates, thus resulting in increasing both population vital rates.

While almost all of the parameters in the model could be estimated from studies of *G. monostachia* populations in Costa Rica [3, 4] or mathematical relationships with those estimated parameters, one parameter could not. The proportion of seeds each year that land in a location suitable for germination after dispersal (h) is not estimated within the literature. To understand the impact of this unknown parameter on the population growth rate, the value of the proportion h was varied over 99% of its feasible range, specifically from 1% ($h = 0.01$) to 100% ($h = 1$). Our analysis showed that the dominant eigenvalue increases as h increases, and thus a *G. monostachia* population with a low proportion of seeds that disperse to a suitable location for germination will have a difficult (or potentially impossible) time remaining viable when experiencing high reductions in survival rates due to weevil predation. Given that the Florida *G. monostachia* populations have been reduced in size since the

1990s due to weevil predation [8], our analysis suggests that either the survival rates have been drastically reduced (if $h > 0.1$) or there have only been moderate reductions in survival rates, but the proportion of seeds that land in a suitable location for germination is very low ($h < 0.1$). If future research is able to estimate a range for h for *G. monostachia* populations, then our model, in conjunctions with *G. monostachia* demographic data, could be used to estimate the potential range of reductions in survival and clonal fecundity rates due to weevil predation.

Appendix

Constrained LHS

Let x and y be parameters that can be sampled from defined distributions $\mathcal{X}$ and $\mathcal{Y}$, respectively, which may overlap. Let $\mathbf{x}$ and $\mathbf{y}$ be column vectors of length n containing sampling from $\mathcal{X}$ and $\mathcal{Y}$, respectively, generated using Latin hypercube sampling (LHS, see [1] for details). For any particular sampling pair (x_i, y_i) we wish to satisfy the constraint

$$x_i > y_i. \tag{3}$$

Petelet et al. provide the necessary and sufficient condition for the existence of at least one such permutation of $\mathbf{y}$, called $\mathbf{y}^*$, such that $x_i > y_i^*$ for all i [14, Equation (9)]. Additionally, Petelet et al. [14] provide an algorithm for finding such a permutation of $\mathbf{y}$.

Necessary & sufficient existence condition: Let $\mathbf{C}$ be a matrix such that $c_{ij} = 1$ if $x_j > y_i$ and $c_{ij} = 0$ otherwise, where $\mathbf{C}$ is known as the compatibility matrix. Let $\mathbf{S}$ be a column vector such that $s_i = \sum_{j=1}^{n} c_{ij}$, that is s_i is the sum across each row of $\mathbf{C}$. If

$$\text{sort}(\mathbf{S}) - \begin{bmatrix} 1 \\ \vdots \\ n \end{bmatrix} \geq \begin{bmatrix} 0 \\ \vdots \\ 0 \end{bmatrix}, \tag{4}$$

then there exists a permutation of $\mathbf{y}$, called $\mathbf{y}^*$, such that $x_i > y_i^*$ for all i.

Algorithm for finding $\mathbf{y}^*$: Given vectors $\mathbf{x}$ and $\mathbf{y}$ that meet the necessary and sufficient existence condition defined above, the following algorithm produces a permutation of $\mathbf{y}$, denoted as $\mathbf{y}^*$ such that $x_i > y_i^*$ for all i.

1. Run an LHS algorithm to find $\mathbf{x}$ and $\mathbf{y}$.
2. Let $\mathbf{C}^* = \mathbf{C}$, $\mathbf{b}^* = \mathbf{0}$ (a row vector of length n), and $\mathbf{a}^*$ be a row vector of length n where a_{ij} is the position of the i^{th} smallest element of $\mathbf{x}$.
3. For $k = 1, \ldots, n$,
   - Set $j = a_k^*$
   - Form $\mathbf{b}$, an array of the indices of column j of $\mathbf{C}^*$ that are equal to 1
   - Set $r = \text{rand}(\mathbf{b})$
   - Set $b_j^* = r$
   - Set all the elements of row r of $\mathbf{C}^*$ equal to 0
4. Let $\mathbf{y}^*$ be the permuation of $\mathbf{y}$ according to $\mathbf{b}^*$, i.e. $y_k^* = y_{b_k^*}$ for all $k = 1, \ldots, n$.

Author Contributions

H. Pennington, P. Lingareddy, and E. N. Bodine designed the model, conducted the literature review necessary to parameterize the model, analyzed the model outputs and uncertainty analysis, and wrote this resulting manuscript. H. Pennington and P. Lingareddy implemented the model, LHS and cLHS sampling methods, and uncertainty analysis in Matlab. E. N. Bodine created the *G. monostachia* sketches shown in Figure 1.

References

[1] Blower, S. and Dowlatabadi, H. (1994). Sensitivity and uncertainty analysis complex models of disease transmission: an HIV model, as an example. *International Statistical Review / Revue Internationale De Statistique*, 62(2):229–243.

[2] Brookover, Z., Campbell, A., Christman, B., Davis, S., and Bodine, E. (2020). A demographic model of an endangered Florida native bromeliad (*Tillandsia utriculata*). *Spora*, 6(2):1–15.

[3] Cascante-Marín, A., Jong, M., Oostermeijer, J., Wolf, J., Borg, E., and Nijs, J. (2006). Reproductive strategies and colonizing ability of two sympatric epiphytic bromeliads in a tropical premontane area. *International Journal of Plant Sciences*, 167(6):1187–1195.

[4] Cascante-Marín, A., Oostermeijer, J., Wolf, J., and Nijs, J. (2008). Establishment of epiphytic bromeliads in successional tropical premontane forests in Costa Rica. *Biotropica*, 40(4):441–448.

[5] Cascante-Marín, A., von Meigenfeldt, N., de Leeuw, H., Wolf, J., Oostermeijer, J., and den Nijs, J. (2009). Dispersal limitation in epiphytic bromeliad communities in a Costa Rican fragmented montane landscape. *Journal of Tropical Ecology*, 25:63–73.

[6] Caswell, H. (2001). *Matrix Population Models: Construction, Analysis, and Interpretation*. Sinauer.

[7] Cooper, T. (2006). Ecological and demographic trends and patterns of *Metamasius callizona* (chevrolat), an invasive bromeliad-eating weevil, and Florida's native bromeliads. Master's thesis, University of Florida.

[8] Cooper, T. (2016). Florida's native bromeliads: *Guzmania monostachnia*. Technical report, University of Florida Institute of Food and Agrigultural Sciences. Available at `https://entnemdept.ufl.edu/frank/savebromeliads/floridas-bromeliads/Guzmania-monostachia.html`.

[9] Frank, H. and Cave, R. (2005). *Metamasius callizona* is destroying Florida's native bromeliads. In *Second International Symposium on Biological Control of Arthropods, Davos, Switzerland*, pages 91–101.

[10] Kot, M. (2001). *Elements of Mathematical Ecology*. Cambridge University Press, Cambridge, UK.

[11] Larson, B. and Frank, J. (2019). Mexican bromeliad weevil (suggested common name), *Metamasius callizona* (chevrolat) (insecta: Coleoptera: Curculionidae). Technical report, Entomology and Nematology Department, University of Florida Institution of Food & Agricultural Sciences (UF/IFAS) Extension.

[12] Luther, H. and Benzing, D. (2009). *Native Bromeliads of Florida*. Pineapple Press, Sarasota, FL.

[13] McKay, M., Beckman, R., and Conover, W. (1979). A comparison of three methods for selecting values of input variables in the analysis of output from a computer code. *Technometrics*, 21(2):239–245.

[14] Petelet, M., Iooss, B., Asserin, O., and Loredo, A. (2010). Latin hypercube sampling with inequality constraints. *AStA Advances in Statistical Analysis*, 94(1):325–339.

[15] Weaver, R. and Anderson, P. (2010). Notes on Florida's endangered and threatened plants, 5^{th} edition. Technical Report 38, Bureau of Entomology, Nematology, and Plant Pathology—Botany Section. Available at `https://www.fdacs.gov/ezs3download/download/92005/2597881/Media/Files/Plant-Industry-Files/FLORIDAS-ENDANGERED-AND-THREATENED-PLANTS.pdf`.